Hindawi Publishing Corporation
Journal of Radiotherapy
Volume 2014, Article ID 760206, 7 pages
http://dx.doi.org/10.1155/2014/760206

Clinical Study

Dosimetric Studies of Mixed Energy Intensity Modulated Radiation Therapy for Prostate Cancer Treatments

K. Abdul Haneefa,[1] K. K. Shakir,[2] A. Siddhartha,[2] T. Siji Cyriac,[3,4] M. M. Musthafa,[5] and R. Ganapthi Raman[4]

[1] *INFN and Department of Physics, University of Torino, Via P.Giuria, 10125 Torino, Italy*
[2] *Department of Radiation Therapy, AJ Cancer Institute, Mangalore, Karnataka 575004, India*
[3] *Department of Radiation Therapy, HCG, Dr.Balabhai Nanavati Hospital, Vile Parle (West), Mumbai, Maharashtra 400 056, India*
[4] *Department of Physics, Noorul Islam Centre for Higher Education, Kumaracoil, Thuckalay, Kanyakumari District, Tamil Nadu 629180, India*
[5] *Department of Physics, University of Calicut, Thenhipalam, Malappuram, Kerala 673635, India*

Correspondence should be addressed to K. Abdul Haneefa; abdul.haneefa@gmail.com

Received 30 November 2013; Revised 1 February 2014; Accepted 11 February 2014; Published 16 March 2014

Academic Editor: Carlos A. Perez

Dosimetric studies of mixed field photon beam intensity modulated radiation therapy (IMRT) for prostate cancer using pencil beam (PB) and collapsed cone convolution (CCC) algorithms using Oncentra MasterPlan treatment planning system (v. 4.3) are investigated in this study. Three different plans were generated using 6 MV, 15 MV, and mixed beam (both 6 and 15 MV). Fifteen patients with two sets of plans were generated: one by using PB and the other by using CCC for the same planning parameters and constraints except the beam energy. For each patient's plan of high energy photons, one set of photoneutron measurements using solid state neutron track detector (SSNTD) was taken for this study. Mean percentage of $V_{66\,\mathrm{Gy}}$ in the rectum is 18.55 ± 2.8, 14.58 ± 2.1, and 16.77 ± 4.7 for 6 MV, 15 MV, and mixed-energy plans, respectively. Mean percentage of $V_{66\,\mathrm{Gy}}$ in bladder is 16.54 ± 2.1, 17.42 ± 2.1, and 16.94 ± 41.9 for 6 MV, 15 MV, and mixed-energy plans, respectively. Mixed fields neutron contribution at the beam entrance surface is 45.62% less than at 15 MV photon beam. Our result shows that, with negligible neutron contributions, mixed field IMRT has considerable dosimetric advantage.

1. Introduction

Radiation therapy (RT), either alone or in combination with chemotherapy and/or surgery, plays a major role in treating prostate cancer. Deep-seated prostate cancer is the second common cancer in men [1, 2], which is widely treated with intensity modulated radiation therapy (IMRT) technique with minimal dose to surrounding organs at risk (OAR).

High energy beams are used for 3-dimensional conformal radiation therapies to treat prostate, while 6 MV, low photon energy is used in IMRT. With a higher surface dose from low energy, low dose gradient and higher conformity are achieved at planning target volumes to minimize bladder and rectal dose [3–5]. Femoral heads receive higher dose in 3D-CRT and low energy IMRT beams, if the beam angle is not well optimized [6]. High energy is always limited in IMRT because of the probability of photoneutron production, where multileaf collimators (MLC) are continuously moved during the treatment, and higher beam on time (MU) is required [7, 8].

Treatment planning systems (TPS) optimization gives conformity in the target region [9–11]. To achieve tolerable radiation in the rectum and bladder within the dose constraints given, TPS will optimize the dose fluence at the target. MLC positions and monitor units are generated by these conditions. Modern linacs are given the choice to select two or three optimization algorithms in a single TPS to get an appropriate plan in individual treatments.

Many studies [12–15] postulate no clinical advantages to use high energy (>10 MV) in prostate cancer treatments.

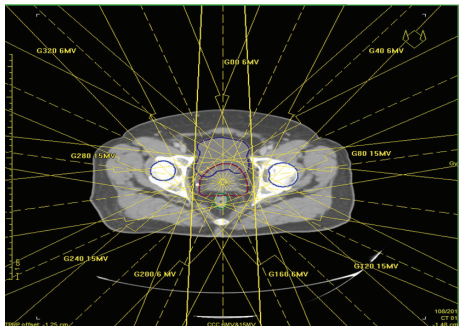

Figure 1: Axial slice showing beam orientation of nine-field IMRT with gantry angle and beam energy.

Wide acceptance of low energy in IMRT is due to the dose conformity and to avoid the risk of photoneutron productions. The adverse effect of low energy includes higher peripheral dose due to complex treatment plans and higher delivery time. Multiple gantry angles will add the integral dose to a great extent [16, 17].

It is felt that the combination of mixed beam can produce better conformity and patient safety; therefore study of dosimetric effects of using a mixed energy beam for prostate IMRT with proper conclusions based on optimization algorithms is carried out. Dosimetric plan evaluations are carried in 6 MV and 15 MV and mixed energy beams plans are studied. Higher energy beams were selected for larger penetration depths and using the low energy was selected for low penetrating regions to achieve desirable dose. A detailed study was performed using two sets of plans, pencil beam and collapsed cone convolution algorithms. Moreover, neutron measurements in mixed energy beam and high energy beam are studied using CR-39 (Columbia resin) neutron track detector in water equivalent plastic phantom.

2. Materials and Methods

Fifteen patients' plans with histopathologically confirmed prostate cancer are considered in the present study. 2 mm sliced CT (computed tomography) was taken for all patients for simulation and planning in Oncentra MasterPlan (v. 4.3). A standard dose 78 Gy (Gray) in 39 fractions (2 Gy/fraction) is delivered to treat the prostate and/or seminal vesicles using IMRT technique. All patients are informed about the acute and late effects and they obtain the consent through the research ethic committee of our institute (AJ Cancer Institute-Kuntikana, Mangalore, India).

2.1. Contouring. In all patients, the body was automatically contoured from our TPS, while all organs are manually drawn in the CT images acquired from CT simulator (GE Lightspeed, GE Healthcare, Chalfont St. Giles, UK) with full bladder condition. Studies are done with low and medium risk patients, so the CTV (clinical target volume) involves only prostate. PTV (planning target volume) was created by expanding 1 cm in all directions except posterior, where 7 mm margin from CTV is considered to reduce the dose to critical organ rectum. Critical organs like bladder, rectum, and femoral heads are drawn for all planes using RTOG-0815 (radiation therapy oncology group) protocol.

Table 1: Mean CTV minimum and maximum values obtained in two algorithms (collapsed cone convolution and pencil beam).

(a)

	CCC			
	6 MV	15 MV	Mixed energy	P
	(Mean ± SD)			
CTVmin	70.56 ± 3.16	69.02 ± 1.71	71.04 ± 2.09	<0.043
CTVmax	90.97 ± 2.04	88.71 ± 3.01	90.05 ± 1.8	<0.05
CI	1.212 ± 0.04	1.129 ± 0.05	1.253 ± 0.03	<0.06
HI	1.189 ± 0.02	1.160 ± 0.02	1.177 ± 0.03	<0.056

(b)

	PB			
	6 MV	15 MV	Mixed energy	P
	(Mean ± SD)			
CTVmin	74.94 ± 3.02	70.21 ± 2.21	72.76 ± 2.54	<0.061
CTVmax	92.74 ± 2.1	90.31 ± 3.67	91.55 ± 3.09	<0.047
CI	1.257 ± 0.05	1.210 ± 0.05	1.314 ± 0.04	<0.07
HI	1.2131 ± 0.03	1.181 ± 0.04	1.197 ± 0.04	<0.066

Minimum and maximum dose to CTV (CTVmin, CVTmax), mean conformity index (CI) and homogeneity index (HI) of the plan are shown in the table with their statistical significance (P).

2.2. Treatment Planning. Oncentra MasterPlan (v. 4.3) is used to generate IMRT plans using two algorithms—pencil beam and collapsed cone convolution. Elekta Synergy Platform (ELEKTA, West Sussex, UK) dual energy (6 and 15 MV) linear accelerator is used for all measurements. Multileaf collimators with 40 leaves (total 80 leaves) on each side make IMRT feasible. Total treatment lasts for 39 days with 2 Gy per fraction. All plans are created by single medical physicist, to reduce possible individual errors.

All plans are generated with unique constraints for PTV and critical organs for this study (actual treatment plans are different from the one used for our study). 95–105% PTV dose uniformity was planned with the initial constraints [18] usually given in our department. Nine- field IMRT with 0°, 40°, 80°, 120°, 160°, 200°, 240°, 280°, and 320° gantry angles is used for all plans. Beam orientation with gantry angle and beam energy is shown in Figure 1. Four gantry (80°, 160°, 240°, and 280°) orientations are with 15 MV in mixed-energy plans, where the photon beams have longer distance to isocenter from the skin surface.

2.3. Dosimetric Evaluation. Dose homogeneity in the PTV for all plans was performed to ensure the plan adequacy and acceptance [19]. Metrics for the homogeneity index (HI) and conformity index (CI) proposed by RTOG (radiation therapy

Table 2: Dose volume comparison for three plans (6 MV, 15 MV, and mixed energy) in two algorithms.

Volume	Cone collapsed convolution				Pencil beam			
	6 MV	15 MV	Mixed energy	Avg. P	6 MV	15 MV	Mixed energy	Avg. P
	(Mean ± standard dose)				(Mean ± standard dose)			
PTV								
MaxDose (Gy)	90.93 ± 2.4	88.41 ± 3.1	90.05 ± 1.2	0.036	92.34 ± 1.7	90.31 ± 1.3	91.45 ± 1.9	0.034
MinDose (Gy)	70.06 ± 2.8	67.20 ± 2.5	69.28 ± 0.8	0.029	71.09 ± 0.8	68.09 ± 2.5	70.36 ± 1.4	0.051
AvgDose (Gy)	79.22 ± 3.6	79.12 ± 3.7	80.45 ± 2.1	0.015	80.12 ± 0.5	80.21 ± 2.2	81.23 ± 1.1	0.013
Rectum								
V66 Gy (%)	18.55 ± 2.8	14.58 ± 2.1	16.77 ± 4.7	0.034	19.05 ± 2.8	15.09 ± 1.7	17.26 ± 4.6	0.048
V40 Gy (%)	42.36 ± 3.1	40.04 ± 1.7	39.53 ± 2.8	0.062	43.23 ± 3.3	38.58 ± 2.8	40.16 ± 2.9	0.058
V20 Gy (%)	60.32 ± 4.6	57.83 ± 2.9	58.55 ± 3.6	0.041	60.65 ± 1.4	58.04 ± 4.0	58.87 ± 3.1	0.031
D50% (Gy)	33.19 ± 2.3	27.21 ± 0.09	31.20 ± 2.9	0.052	33.73 ± 2.6	27.94 ± 3.5	31.54 ± 2.5	0.05
Bladder								
V66 Gy (%)	16.54 ± 2.1	17.42 ± 2.1	16.94 ± 1.9	0.022	16.77 ± 3.6	17.90 ± 2.9	17.58 ± 2.1	0.026
V40 Gy (%)	42.01 ± 3.6	41.77 ± 1.8	42.74 ± 4.2	0.028	43.23 ± 3.1	43.06 ± 4.0	43.39 ± 3.2	0.003
V20 Gy (%)	76.29 ± 3.2	75.66 ± 2.6	75.00 ± 3.8	0.008	76.29 ± 1.2	75.97 ± 1.9	75.01 ± 2.8	0.009
D50% (Gy)	35.54 ± 2.9	34.87 ± 0.9	35.02 ± 2.4	0.010	37.58 ± 4.6	35.50 ± 3.4	35.06 ± 2.9	0.034
Femoral heads								
V20 Gy (%)	84.84 ± 5.4	84.03 ± 3.9	83.12 ± 4.2	0.041	84.26 ± 3.6	84.68 ± 2.9	83.55 ± 4.3	0.029
D50% (Gy)	25.04 ± 3.4	25.06 ± 2.5	24.28 ± 1.9	0.029	25.84 ± 2.7	25.06 ± 1.4	24.69 ± 3.1	0.032
Monitor units								
AvgMU	755 ± 10.6	655 ± 11.58	776 ± 8.4	0.035	742 ± 12.3	654 ± 10.46	777 ± 13.5	0.028

Avg.: average; MaxDose: maximum dose; MinDose: minimum dose; AvgDose: average dose; and MU: monitor units.

Table 3: Mean photoneutron track density and neutron dose (calibration constant of 1.2 tracks/mSv) at surface and isocenter depths for 15 MV and mixed energy beams for 0° gantry angles.

	15 MV			Mixed energy		
	Surface	Isocenter	P	Surface	Isocenter	P
	(Mean ± SD)			(Mean ± SD)		
Track density (1/cm^3)	175.5 ± 12.7	62 ± 6.2	0.137	111 ± 17.8	46.8 ± 9.3	0.093
Neutron dose (mSv)	146.25 ± 10.58	51.66 ± 5.16	0.097	92.5 ± 14.83	39 ± 7.75	0.085

oncology group) are used to assess the quality of treatment plan that is shown in (1) and (2), respectively,

$$\mathrm{HI} = \frac{I_{\mathrm{MAX}}}{\mathrm{RI}}. \quad (1)$$

Here, I_{MAX} is the maximum isodose in the target and RI is reference isodose (76.45 Gy):

$$\mathrm{CI} = \frac{V_{\mathrm{RI}}}{\mathrm{TV}}. \quad (2)$$

Here, V_{RI} is the volume of reference isodose and TV is the target volume.

The maximum, minimum, and the mean doses of the PTV, rectum, bladder, and femoral heads are calculated for all plans. Tissue volumes in all the critical organs (rectum, bladder, and femoral heads) receiving 66 Gy, 40 Gy, and 20 Gy are evaluated in all plans for both algorithms. All above doses (maximum, minimum, and mean) and volumes of definite doses described are compared with Student's t-test (dependent) sampling method with P value of <0.05 that is accepted for statistical significance [18, 20].

2.4. Neutron Measurements. Photoneutrons are measured using CR-39 SSNTD (solid state neutron track detector) for high energy and mixed-energy plans in uniform water equivalent phantom for single fraction at isocenter distance with gantry angle merged to zero degree. Films (Intercast Europe S.p.A, Italy) are etched (track forming) in 6.25 N NaOH solution for 8 hours at 70°C [21]. Neutron tracks are counted using Olympus microscope with 1000x zooming. The calibration constant for these films is taken as 1.2 tracks/mSv [22].

3. Results and Discussion

Mean CTV minimum and maximum dose values for pencil beam and collapsed cone convolution plans are shown in Table 1. Mean difference of 2.5% is found in CTV minimum dose values for 6 and high energy beams. Mean difference of 1.0% is found in between 6 and mixed beam IMRTs in both algorithms. Mean values of RTOG metrics for homogeneity and conformity index for all plans are given in Table 1.

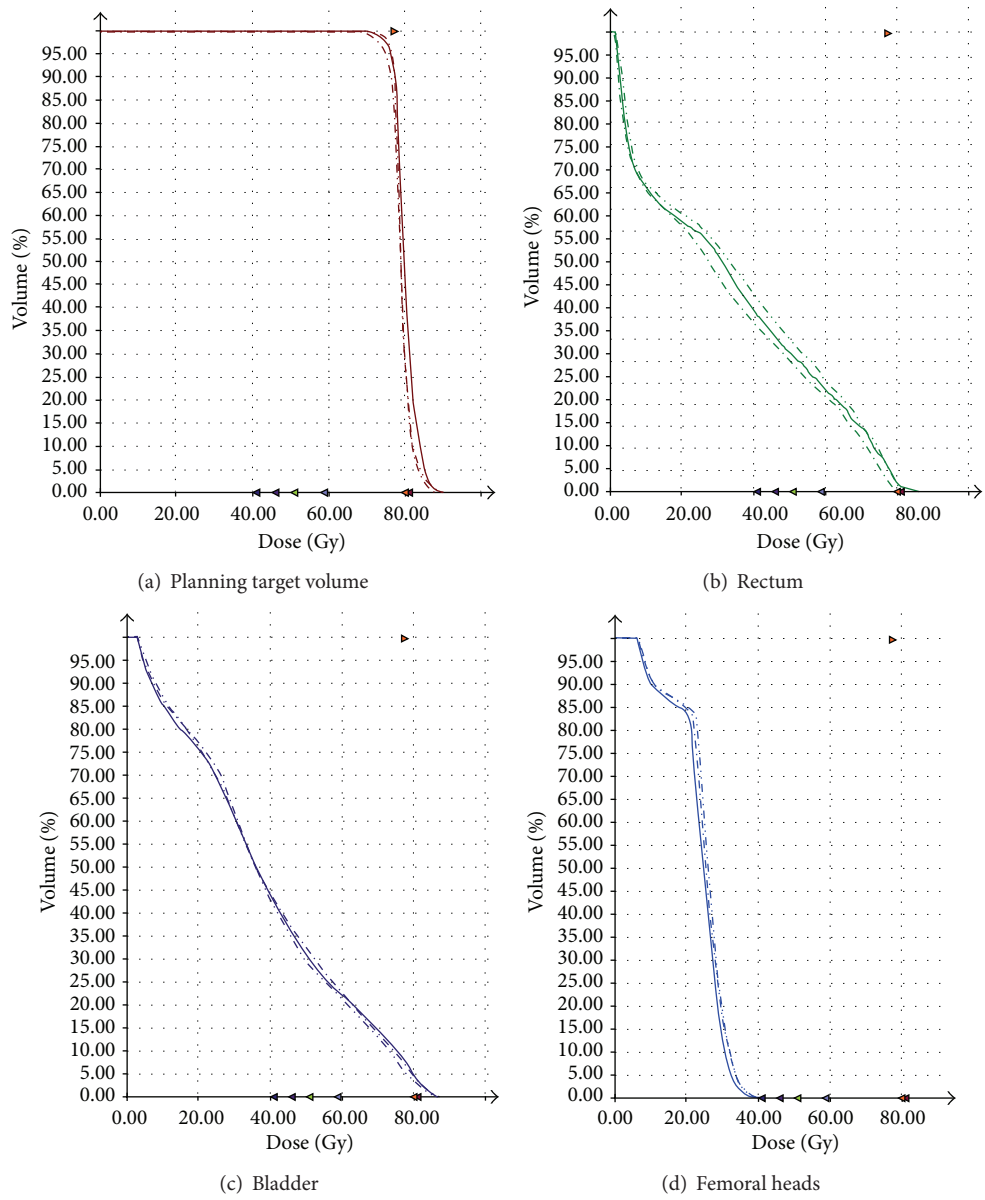

Figure 2: Dose volume histograms (DVHs) of PTV for three-type plans (6 MV, 15 MV, and mixed energy) in CCC algorithm: (a) DVH for PTV; (b) DVH for rectum; (c) DVH for bladder; and (d) DVH for femoral heads. The solid line represents DVH for mixed energy, the dotted line represents 15 MV DVH, and the dashed line represents the DVH for 6 MV.

No significant difference in CI and HI is found for both algorithms.

Typical dose volume histogram (of single patient) for PTV, rectum, bladder, and femoral heads in CCC algorithm is shown in Figure 2. The solid line represents DVH for mixed energy, the dotted line represents 15 MV DVH, and the dashed line represents the DVH for 6 MV. Detailed dose volumetric studies for PTV and OARs are shown in Table 2. The mean percentage of the volume receiving 20 Gy ($V_{20\,\mathrm{Gy}}$), 40 Gy ($V_{40\,\mathrm{Gy}}$), and 66 Gy ($V_{66\,\mathrm{Gy}}$) is analyzed for all OARs (rectum and bladder and right and left femoral heads). Figure 3 shows the isodose distributions for low, high, and mixed-energy plans in axial, sagittal, and coronal planes using CCC algorithm. Mixed energy isodose curves show excellent coverage than low energy plan with minimum involvement of surrounding critical organs.

No significant difference is found in the mean average dose (AvgDose) in PTV for both algorithms. However slightly better PTV dosage is found in high energy IMRT for mean maximum dose (MaxDose) and mean minimum dose (MinDose) than in 6 MV and mixed energy IMRTs in both algorithms.

For rectum mean $V_{66\,\mathrm{Gy}}$ in mixed energy IMRT is 10.07% less than 6 MV IMRT and 13.9% higher than 15 MV IMRT using CCC algorithm. In CCC mean $V_{40\,\mathrm{Gy}}$ in the mixed energy IMRT is 6.7% less than 6 MV IMRT. For mean $D_{50\%}$ in mixed energy IMRT is 6.2% less than 6 MV and 13.66% higher than 15 MV IMRT. No significant difference is

(a) Mixed energy (6 and 15 MV) isodose distribution

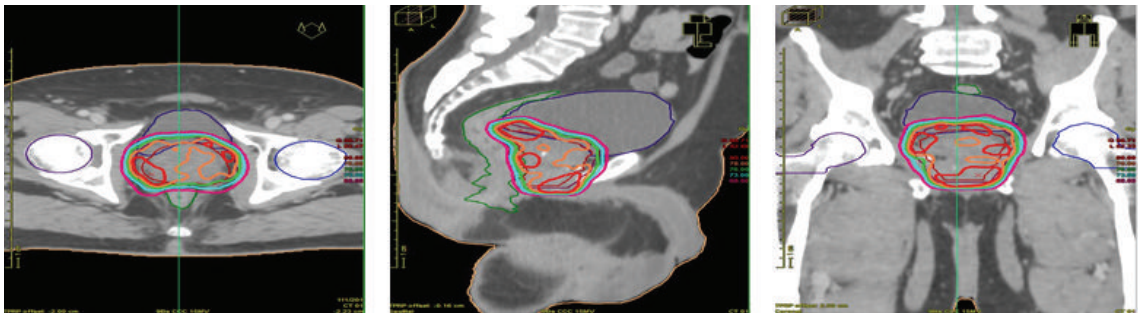

(b) High energy (15 MV) isodose distribution

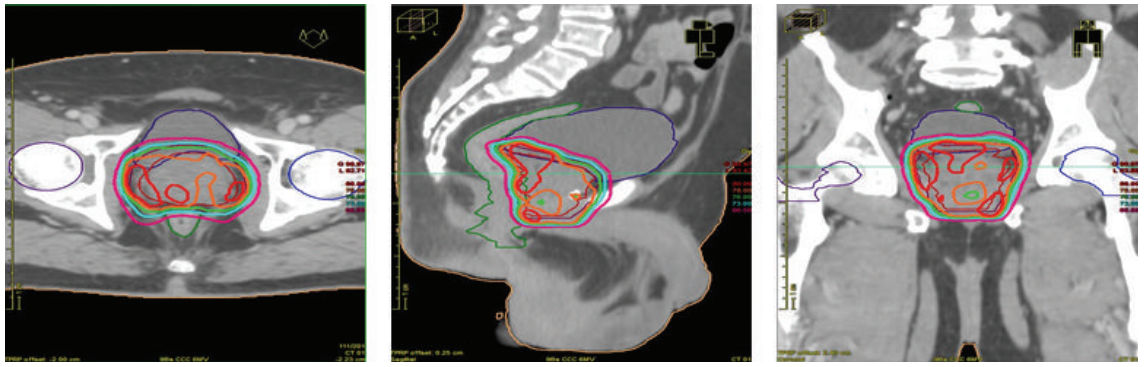

(c) Low energy (6 MV) isodose distribution

Figure 3: The isodose distributions for low, high, and mixed-energy plans in axial, sagittal, and coronal planes using CCC algorithm.

found in CCC and PB algorithms. Slightly better dosimetric conformities are achieved in 15 MV and mixed energy IMRTs for minimal dose to rectum.

High energy and mixed energy IMRTs always show lower doses to bladder in both algorithms. Mean $V_{40\,\mathrm{Gy}}$ is considerably lower in mixed-energy plans than 6 and 15 MV IMRTs. No significant difference in three IMRT plans for $V_{20\,\mathrm{Gy}}$ is observed in both algorithms. $V_{66\,\mathrm{Gy}}$ is slightly (2.7%) less in 15 MV IMRT than in mixed energy IMRT in CCC. $D_{50\%}$ in both algorithms has a mean difference of 2.7% lower in mixed energy than in 6 MV IMRT.

Mean $V_{20\,\mathrm{Gy}}$ for femoral heads is slightly improved in mixed energy IMRT than in 15 MV and 6 MV IMRTs. Only 2% difference in $D_{50\%}$ is found in mixed-energy plans than in 6 and 15 MV plans. CCC and PB show very similar results.

Apart from the larger computing time (20–30%) in PB than in CCC, both algorithms show less dependence in optimization of various plans for prostate cancer IMRT. As shown in previous studies [4, 5, 16, 23, 24], no distinctive difference in dosimetric studies using 6 MV and 15 MV is noticed in our study also. Mixed energy can be included into these features for prostate cancer treatment using nine-field IMRT. Higher surface dose of 6MV photon beam contributes higher dose at femoral head regions; however CCC algorithm shows less dose than in PB because of accurate out-of-field dose calculations in modern algorithms.

For 6 MV IMRT CCC algorithm gives 1.8% larger mean MU than PB algorithm. Mixed energy shows very slight change in mean MU than 6 MV plans in both algorithms, while 28% is mean MU difference which is found between 6 MV and 15 MV IMRT plans.

Average photoneutrons track density in isocenter and surface depth for mixed energy and 15 MV plans are shown in Table 3. Photoneutron dose is 45% less in mixed-energy plans than in 15 MV at beam entrance surface and 27% less at isocenter depth. Due to unavailability of human torso

phantom we confined the studies in PMMA (polymethyl methacrylate) water equivalent slab phantoms for single gantry angles, where all gantry angles are merged to zero degree as in pretreatment verification mode.

IMRT has been advocated to improve the therapeutic ratio by precise dose conformity at PTV and spare the OARs to the maximum possible extent. In prostate treatment, individualized plans with different beam energy can improve the conformity with minimum photoneutron production. Our results suggested that the mixed energy techniques can improve the overall dosimetric quantities in many patients. Photoneutrons are much less in mixed energy while comparing higher energy for better dosimetric conformity. Heterogeneous phantom studies improve the actual treatment conditions for photoneutron study in various depths of OARs.

4. Conclusion

Mixed energy IMRT has a distinct advantage on dosimetric basis as discussed here. Collapsed cone convolution algorithm optimizes the plans better than the pencil beam in mixed energy planning, especially in larger distance from the field edge. No clinically relevant advantage on dose reduction at OARs is noticed in all plans, while the target dose uniformity and conformities in deep-seated prostate treatments using mixed energy planning are slightly better than treating with 6 or 15 MV alone. It is noticed that the neutron measurement of the mixed energy beam is much less than high energy radiation therapy.

Conflict of Interests

The authors declare no conflict of interests.

Acknowledgment

The authors are very grateful to Dr. Kamaleksh Shenoy, radiation oncologist at AJ Cancer Institute, Mangalore, India, for supporting this work apart from routine clinical works.

References

[1] E. J. Hall and A. J. Giaccia, *Radiobiology for the Radiologist*, Lippincott Williams & Wilkins, Philadelphia, Pa, USA, 6th edition, 2006.

[2] M. Beyzadeoglu, G. Ozyigit, and C. Ebruli, *Basic Radiation Oncology*, Springer, Berlin, Germany, 2008.

[3] J. S. Laughlin, R. Mohan, and G. J. Kutcher, "Choice of optimum megavoltage for accelerators for photon beam treatment," *International Journal of Radiation Oncology Biology Physics*, vol. 12, no. 9, pp. 1551–1557, 1986.

[4] G. Solaiappan, G. Singaravelu, A. Prakasarao, B. Rabbani, and S. S. Supe, "Influence of photon beam energy on IMRT plan quality for radiotherapy of prostate cancer," *Reports of Practical Oncology and Radiotherapy*, vol. 14, no. 1, pp. 18–31, 2009.

[5] G. de Meerleer, L. Vakaet, S. Meersschout et al., "Intensity-modulated radiotherapy as primary treatment for prostate cancer: acute toxicity in 114 patients," *International Journal of Radiation Oncology Biology Physics*, vol. 60, no. 3, pp. 777–787, 2004.

[6] A. Pollack, A. Hanlon, E. M. Horwitz, S. Feigenberg, R. G. Uzzo, and R. A. Price, "Radiation therapy dose escalation for prostate cancer: a rationale for IMRT," *World Journal of Urology*, vol. 21, no. 4, pp. 200–208, 2003.

[7] R. M. Howell, N. E. Hertel, Z. Wang, J. Hutchinson, and G. D. Fullerton, "Calculation of effective dose from measurements of secondary neutron spectra and scattered photon dose from dynamic MLC IMRT for 6 MV, 15 MV, and 18 MV beam energies," *Medical Physics*, vol. 33, no. 2, pp. 360–368, 2006.

[8] National Council on Radiation Protection and Measurements, "Neutron contamination from medical electron accelerators," NCRP Report 79, NCRP, Bethesda, Md, USA, 2009.

[9] C. Burman, C. S. Chui, G. Kutcher et al., "Planning, delivery, and quality assurance of intensity-modulated radiotherapy using dynamic multileaf collimator: a strategy for large-scale implementation for the treatment of carcinoma of the prostate," *International Journal of Radiation Oncology Biology Physics*, vol. 39, no. 4, pp. 863–873, 1997.

[10] G. E. Hanks, A. L. Hanlon, T. E. Schultheiss et al., "Dose escalation with 3D conformal treatment: five year outcomes, treatment optimization, and future directions," *International Journal of Radiation Oncology Biology Physics*, vol. 41, no. 3, pp. 501–510, 1998.

[11] J. H. Mott, J. E. Livsey, and J. P. Logue, "Development of a simultaneous boost IMRT class solution for a hypofractionated prostate cancer protocol," *British Journal of Radiology*, vol. 77, no. 917, pp. 377–386, 2004.

[12] M. Sun and L. Ma, "Treatment of exceptionally large prostate cancer patients with low-energy intensity-modulated photons," *Journal of Applied Clinical Medical Physics*, vol. 7, no. 4, pp. 43–49, 2006.

[13] T. S. Subramanian, J. P. Gibbons Jr., and W. R. Hendee, "Linear accelerators used for IMRT should be designed as small field, high intensity, intermediate energy units," *Medical Physics*, vol. 29, no. 11, pp. 2526–2528, 2002.

[14] M. J. Zelefsky, Z. Fuks, L. Happersett et al., "Clinical experience with intensity modulated radiation therapy (IMRT) in prostate cancer," *Radiotherapy and Oncology*, vol. 55, no. 3, pp. 241–249, 2000.

[15] L. J. Bos, M. Schwarz, W. Bär et al., "Comparison between manual and automatic segment generation in step-and-shoot IMRT of prostate cancer," *Medical Physics*, vol. 31, no. 1, pp. 122–130, 2004.

[16] M. Sun and L. Ma, "Treatment of exceptionally large prostate cancer patients with low-energy intensity-modulated photons," *Journal of Applied Clinical Medical Physics*, vol. 7, no. 4, pp. 43–49, 2006.

[17] S. Söderström, A. Eklöf, and A. Brahme, "Aspects on the optimal photon beam energy for radiation therapy," *Acta Oncologica*, vol. 38, no. 2, pp. 179–187, 1999.

[18] J. M. Park, C. H. Choi, S. W. Ha, and S. J. Ye, "The dosimetric effect of mixed-energy IMRT plans for prostate cancer," *Journal of Applied Clinical Medical Physics*, vol. 12, no. 4, pp. 147–157, 2011.

[19] Q. Wu, R. Mohan, M. Morris, A. Lauve, and R. Schmidt-Ullrich, "Simultaneous integrated boost intensity-modulated radiotherapy for locally advanced head-and-neck squamous cell carcinomas. I: dosimetric results," *International Journal of Radiation Oncology Biology Physics*, vol. 56, no. 2, pp. 573–585, 2003.

[20] B. Uysal, M. Beyzadeoğlu, Ö. Sager et al., "Dosimetric evaluation of intensity modulated radiotherapy and 4-field 3-D conformal radiotherapy in prostate cancer treatment," *Balkan Medical Journal*, vol. 30, no. 1, pp. 54–57, 2013.

[21] R. Bedogni, C. Domingo, A. Esposito et al., "Calibration of PADC-based neutron area dosemeters in the neutron field produced in the treatment room of a medical LINAC," *Radiation Measurements*, vol. 50, pp. 78–81, 2013.

[22] D. Sh Al-Othmany, S. Abdul-Majid, and M. W. Kadi, "Fast neutron dose mapping in a linac radiotherapy facility," in *Proceedings of the 10th Radiation Physics & Protection Conference*, pp. 123–128, November 2010.

[23] S. F. de Boer, Y. Kumek, W. Jaggernauth, and M. B. Podgorsak, "The effect of beam energy on the quality of IMRT plans for prostate conformal radiotherapy," *Technology in Cancer Research and Treatment*, vol. 6, no. 2, pp. 139–146, 2007.

[24] A. Pirzkall, M. P. Carol, B. Pickett, P. Xia, M. Roach III, and L. J. Verhey, "The effect of beam energy and number of fields on photon-based IMRT for deep-seated targets," *International Journal of Radiation Oncology Biology Physics*, vol. 53, no. 2, pp. 434–442, 2002.